Available online at www.eccomasproceedia.org
Eccomas Proceedia UNCECOMP (2025) 511-522

ECCOMAS Proceedia

UNCECOMP 2025
6th ECCOMAS Thematic Conference on
Uncertainty Quantification in Computational Science and Engineering
M. Papadrakakis, V. Papadopoulos, G. Stefanou (eds.)
Rhodes Island, Greece, 15-18 June 2025

VIBRATIONS ANALYSIS OF STRUCTURAL PROPERTIES WITH UNCERTAINTIES USING OSCILLATORY PHYSICS-INFORMED NEURAL NETWORKS (OPINN)

Stefan Hildebrand[1], **and Sandra Klinge**[1]

[1] Department of Structural Mechanics and Analysis, Technische Universität Berlin
Straße des 17. Juni 135, 10623 Berlin, Germany
e-mail: {stefan.hildebrand, sandra.klinge}@tu-berlin.de

Abstract. *Physics-Informed Neural Networks (PINN) methods have proven to be highly versatile and have been successfully applied to a broad variety of problems, such as elastostatics, heat transfer, material modeling or fluid flow. For the investigation of vibrations, a novel oscillatory Physics-Informed Neural Network (oPINN) architecture is developed. It allows for a great variety of hybrid Physics-Informed and data-driven analyses of structures, particularly in cases of incomplete or uncertain information about the system properties. In the oPINN framework, sparse or noisy vibration measurements can be integrated with structural modeling to obtain an accurate and comprehensive system representation. Additionally, estimates of a structure's eigenfrequencies can be included to reduce the computational effort. The oPINN approach achieves accuracy comparable to or exceeding conventional Adams Predictor-Corrector methods. High stability, especially in numerically challenging cases is demonstrated. Transfer learning can significantly enhance computational efficiency for series of similar setups, which might play an important role in parameter studies or multi-frequency excitation analyses. Moreover, oPINN can be employed as a modal reduction technique.*

Keywords: Machine Learning, Physics-Informed, Neural Networks, Vibrations, Oscillations, Elastic continua

doi: 10.7712/120225.12374.21345

1 INTRODUCTION

Many engineering tasks require dynamic simulations of structures, specificall with respect to vibrations. Examples are earthquake engineering, acoustics, failsafe and reliable design of engines and turbines [1, 2, 3], design of bearings [4, 5], brakes [6] and in railway engineering [7]. Currently, the finit element method (FEM) is the standard computational method for transient simulations of oscillating structures. For high frequencies, high-resolution temporal and spatial discretization is required, which makes the simulation computationally challenging [8, 9, 10]. Hyperbolic equations like the wave equation bring challenges to the numerical solution as they often exhibit local nonlinear shock waves while Dahlquist's barriers describe the limitations in regard of stability and accuracy properties of the broad and important class of the linear multistep time-stepping methods [11, 12, 13, 14].

Currently, the use of machine learning (ML) with neural networks (NN) [15, 16, 17] gains increasing attentions in a variety of field due to their ability to universally approximate functions paired with outstanding parallelizability [18, 19]. Among others, very promising results have been presented for modeling of plasticity [20, 21, 22, 23], hyperelasticity and magnetoactivity [24, 25, 26] and steel-reinforced concrete [27]. In the area of physical problems, physics-informed neural networks (PINN) are a promising technique which does not require training data. Instead, the differential equation describing the respective physical phenomena is evaluated and its residual minimized to train the neural network. This way, the network is trained to output the solution of the differential equation at the sample or collocation points given as inputs. Data sources, such as pre-training with measurement data, can be added [28, 29]. For hyperbolic equations, incorporating the method of characteristics [30] has been suggested as well as physics informed attention neural networks (PIANN), which combine recurrent neural networks and attention mechanisms [31]. Similar to conventional time-stepping methods, an artificia viscosity term can be added to the PDE to increase the solution stability [32], whereas the viscosity coefficien ν can be trained as another learnable parameter. Despite these suggestions, the literature on the application of PINNs to dynamic problems largely focuses on test cases with low frequencies [33], since PINNs tend to prioritize learning lower frequency modes, while high-frequency patterns often do not converge. This can be addressed by transfer learning from low-frequency cases towards higher frequency cases [34, 35].

The proposed oPINN architecture adresses this issue primarily by an internal architecture that facilitates the learning with a define range of frequencies and demonstrates superior accuracy and stability compared to the predictor-corrector time-stepping scheme chosen as reference. Moreover, the oPINN architecture allows an easy integration of all known data, such as sparse or noisy measurement data or related simulation results, to improve the accuracy, for acceleration by pre-training and transfer learning. Besides, oPINN can at the same time deliver a modal analysis and with reduced layer width serve as modal reduction, where the eigenfrequencies and eigenshapes of a structure are obtained directly from the NN parameters.

2 GOVERNING EQUATIONS

The wave equation

$$\frac{\partial^2 \boldsymbol{u}}{\partial t^2} - c^2 \Delta \boldsymbol{u} = \boldsymbol{0} \tag{1}$$

with the elastic deflectio $\boldsymbol{u}(\boldsymbol{x}, t)$, the sound velocity c and time t is a hyperbolic equation and applies to both the tensile bar and the string.

The wave speed for the tensile bar is

$$c^2 = \frac{E}{\rho} \tag{2}$$

where E is the Young's modulus and ρ the material density.

The general homogeneous solution of the homogeneous wave equation is [36]:

$$u_h(x,t) = \sum_{j=1}^{\infty} \left(A_j \cos\left(\frac{\omega_j}{c}x\right) + B_j \sin\left(\frac{\omega_j}{c}x\right)\right) \cdot \left(C_j \cos(\omega_j t) + D_j \sin(\omega_j t)\right), \tag{3}$$

$$A_j, B_j, C_j, D_j \in \mathbb{R}.$$

For a system with a force excitation, the particular solution needs to be added to the homogeneous solution to get the general solution. For a harmonic sine force, the particular solution reads

$$u_p(x,t) = \left(E \cos\left(\frac{\Omega}{c}x\right) + F \sin\left(\frac{\Omega}{c}x\right)\right) \sin(\Omega t) \quad . \tag{4}$$

In case of a harmonic cosine excitation, the equation is instead multiplied with $\cos(\Omega t)$. The eigenfrequencies are determined from the homogeneous solution, however, their values depend on the boundary conditions.

A one-sided clamped bar has the following eigenfrequencies [37]:

$$\omega_j = \frac{(2j+1)\pi}{2}\frac{c}{l}, \ j = 0, 1, \dots . \tag{5}$$

The eigenfrequencies for a bar that is fi ed on both ends, as well as for a bar that is free at both ends, are [37]:

$$\omega_j = (j+1)\pi \frac{c}{l}, \ j = 0, 1, \dots . \tag{6}$$

Only the eigenmodes differ for these two cases. In the following, the kinetic and strain energy are employed as a means to evaluate the accuracy of simulation results, since the trade-off between stability and accuracy in conventional time stepping algorithms often is quantifie by the loss in the calculated energy over the simulated time interval. This reduction of energy has a urely numerical character and is often considered as numerical viscosity. The kinetic energy of a tensile bar is [38]

$$E_{kin} = \frac{1}{2}\int_0^l \rho A \dot{u}^2 \mathrm{d}x \tag{7}$$

and the strain energy

$$E_{str} = \frac{1}{2}\int_0^l EAu'^2 \mathrm{d}x \quad . \tag{8}$$

The work done by an excitation force is

$$W_{force}(t) = \int_0^l F(t)\mathrm{d}u. \tag{9}$$

The balance of energy in the oscillating system is given by

$$E_{tot} = E_{kin}(t=0) + E_{str}(t=0) + W_{force}(t) = E_{kin}(t) + E_{str}(t) \quad . \tag{10}$$

3 METHODS AND MATERIALS

3.1 Physics-Informed Neural Networks (PINNs)

NNs with parameter set Θ consisting of the weights w and biases b represent an arbitrary mapping $\mathcal{R} : \mathbb{R}^n \mapsto \mathbb{R}^m$ from the input to the output side, with n and m the input and output layer width, respectively (universal approximation theorem, [39, 40]). For training, gradient descent based optimization algorithms like Adam [41] are used, based on the MSE loss which typically yields robust and accurate results

$$\mathrm{MSE} = \frac{1}{N}\frac{1}{m}\sum_{k=1}^{N}\sum_{i=1}^{m}(R_i(P^k) - \tilde{R}_i(P^k))^2 \quad . \tag{11}$$

Here, P denotes the input to the NN, R the target output and $\tilde{R}$ the actual NN output of dimension m with N entries. In the following, quantities denoted with a tilde indicate NN outputs or quantities that are calculated based on NN outputs. Thus, all quantities with the tilde symbol are implicitly dependent on the NN parameter set Θ.

Data driven methods rely on available measurements and have been, among other scenarios, applied to detect and characterize brake squeal [42], conduct system identificatio of nonlinear oscillators [43], performance analysis of control system structures [44] and the prediction of nonlinear dispersive waves [45]. PINNs, on the contrary, use the underlying physics of a problem formulated as the residual of a partial differential equation (PDE) which is employed as the loss function $\mathcal{L}_{PDE}$ to predict the behavior of a system [28, 46]. Hence, PINNs represent a collocation method which can be used without the need of complex meshes [30].

The boundary conditions can be included in two different ways. One way is to include the boundary term in the loss as $\mathcal{L}_{BC}$, which is called weak enforcement [29]. The total loss then consists of [47]:

$$\mathcal{L} = \mathcal{L}_{PDE} + \mathcal{L}_{BC}. \tag{12}$$

Another method is to ensure that the boundary conditions are fulfille a priori by modifying the NN output [48, 29, 49] which converts the constrained optimization problem into an unconstrained optimization problem

Extensions of PINN include competitive PINN[50] and variational PINN [51]. A variant for solid body mechanics is the deep energy method (DEM) [48, 52] which employs the potential energy of a structure as loss value which has to be minimal in the state of mechanical equilibrium.

3.2 Numerical reference solution method

As reference solution, the widely used Adams predictor-corrector scheme is applied, which allows for a good compromise between stability and accuracy [13]. Specificall , the predictor step is calculated with the second-order Adams-Bashforth method [12]

$$\dot{\tilde{u}}_{t+1} \approx \dot{\tilde{u}}_t + \Delta t\left(\frac{3}{2}\ddot{\tilde{u}}_t - \frac{1}{2}\ddot{\tilde{u}}_{t-1}\right) \quad , \qquad \tilde{u}_{t+1} \approx \tilde{u}_t + \Delta t\left(\frac{3}{2}\dot{\tilde{u}}_t - \frac{1}{2}\dot{\tilde{u}}_{t-1}\right) \tag{13}$$

followed by the corrector step according to the second-order Adams-Moulton method

$$\dot{u}_{t+1} \approx \dot{\tilde{u}}_t + \Delta t\left(\frac{1}{2}\ddot{u}_{t+1} + \frac{1}{2}\ddot{\tilde{u}}_t\right) \quad , \qquad u_{t+1} \approx \tilde{u}_t + \Delta t\left(\frac{1}{2}\dot{\tilde{u}}_{t+1} + \frac{1}{2}\dot{\tilde{u}}_t\right) \quad . \tag{14}$$

The spatial discretization is conducted with central differences of second order and a mesh width of Δx. The temporal discretization is adapted manually until stability is reached.

4 SUGGESTED OSCILLATORY PINN (oPINN) ARCHITECTURE

The custom oPINN architecture with input being the sample coordinates x and time steps t and the output being the displacement u is shown in Fig. 1.

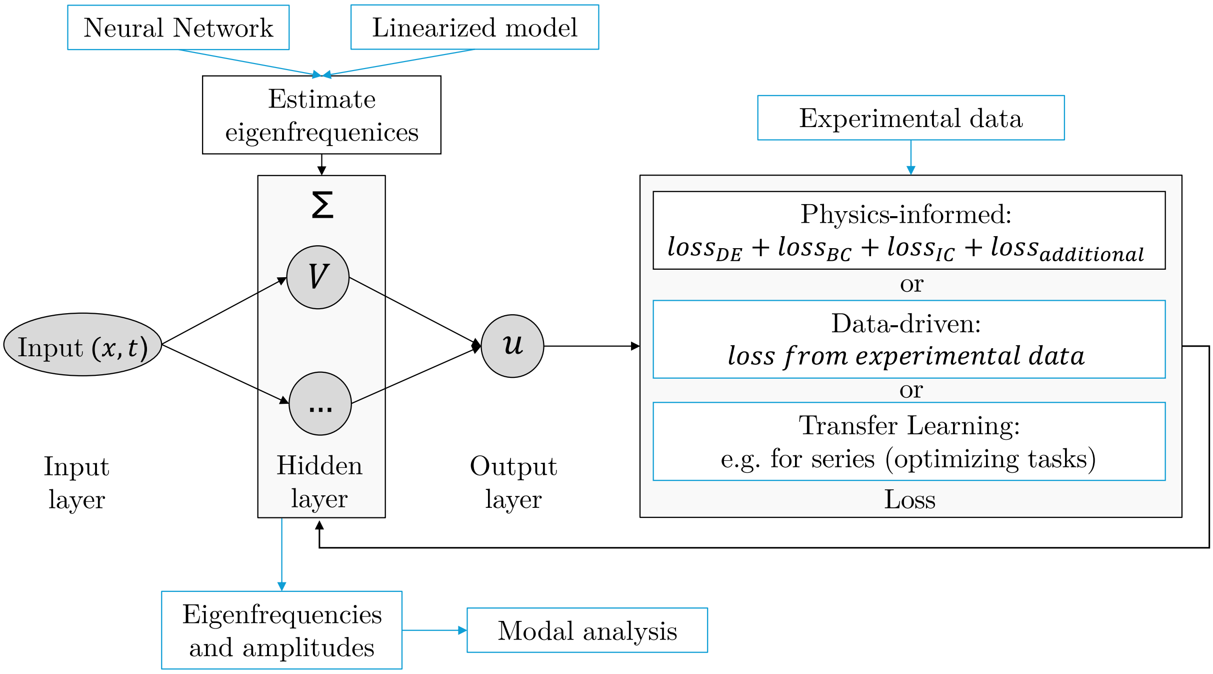

Figure 1: oPINN architecture

Only one hidden layer is used in the network. Harmonic functions are used as activation functions, so that the output of the NN corresponds to the general solution of the wave equation, including the homogeneous solution and the particular solution

$$u(x,t) = \sum_{j=1}^{d} \left(A_j \cos\left(\frac{\omega_j}{c}x\right) + B_j \sin\left(\frac{\omega_j}{c}x\right)\right) \left(C_j \cos(\omega_j t) + D_j \sin(\omega_j t)\right) + P(x,t) \quad , \tag{15}$$

where d is the number of neurons in the hidden layer. The analytical solution has an infinit number of summands. $P(x,t)$ represents the particular solution which in case of a sine excitation is:

$$P(x,t) = \left(E \cos\left(\frac{\Omega}{c}x\right) + F \sin\left(\frac{\Omega}{c}x\right)\right) \sin(\Omega t) \quad . \tag{16}$$

The variables A_j, B_j, C_j, D_j, E, F, ω_j and Ω in Eq. (15) are in this setup the trainable parameters of the oPINN.

These parameters should be initialized in a similar order of magnitude as the corresponding values in the solution. This information can e.g. stem from experience with similar systems, other simplifie simulations, measurements or another data-driven ML application that serves as an estimator. For testing purposes, the initialization values for the eigenfrequencies are drawn from a uniform distribution between 0.5 and 1.5 times the analytical value.

The loss is calculated based on the residual of the wave equation $\mathcal{L}_{PDE}$ and additional terms for the boundary conditions $\mathcal{L}_{BC}$ and initial conditions $\mathcal{L}_{IC}$

$$\mathcal{L} = \mathcal{L}_{PDE} + \lambda_1 \mathcal{L}_{BC} + \lambda_2 \mathcal{L}_{IC} \quad , \tag{17}$$

where the scaling factors λ_i are introduced to weigh the contributions of the loss terms against each other following the considerations from [**?**].

The Dirichlet boundary conditions can be enforced by applying a transformation on the NN output [53, 48]. For the oscillating, left-clamped bar, the boundary condition $u(x = 0, t) = 0$ can be introduced by fixin the constant $A_j = 0$. Then, the general homogeneous solution simplifie to

$$u_h(x, t) = \sum_{j=1}^{hd} B_j \sin\left(\frac{\omega_j}{c} x\right) \left(C_j \cos(\omega_j t) + D_j \sin(\omega_j t)\right) \quad . \tag{18}$$

For the training, the Adam optimizer is employed with learning rate decay halving the learning rate every 100 epochs to refin the solution[54, 55]. As default values, 3000 time step samples in an interval of $1.5\,\mathrm{s}$, an equidistant spatial discretization with 50 sample points and 20 neurons are used. Changes on these default values are indicated explicitly in the following.

5 CASE STUDY – Sawtooth displacement of a tensile bar

The case study presented here is chosen to be maximally challenging for a conventional numerical timestepper, as it deals with the sawtooth displacement movement which in the analytic solution leads to infinitel high frequencies.

It can be produced, when a tensile bar clamped on the left hand side is deformed linearly in its initial state as shown in Fig. 2. The bar has the length $l = 1\,\mathrm{m}$ and is made out of a material with Young's modulus $E = 10\frac{N}{m^2}$ and density $\rho = 1\frac{kg}{m^3}$. The initial deformation at the right end is specifie as $u(x = l, t = 0) = 0.1\,\mathrm{m}$ and the initial displacement is linearly distributed over the length of the bar. After the application of the deformation at $t = 0\,\mathrm{s}$, the bar oscillates freely. This is equivalent to a system that is deformed by a force applied at time $t = 0\,\mathrm{s}$ and removed immediately afterwards.

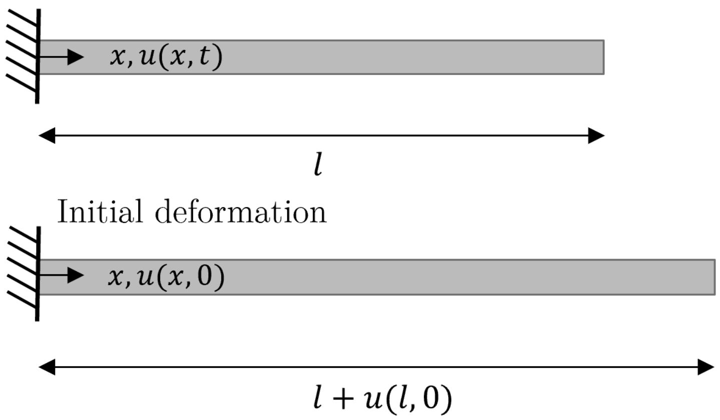

Figure 2: Case study – a tensile bar with an initial linear deformation.

The analytical solution for this case reads

$$u(x,t) = \frac{2F}{EAl} \sum_{j=0}^{\infty} \frac{(-1)^j}{\lambda_j^2} \cos(\omega_j t) \sin(\lambda_j x) \quad . \tag{19}$$

Approximations to this solution with different numbers of summands are visualized in Fig. 3.

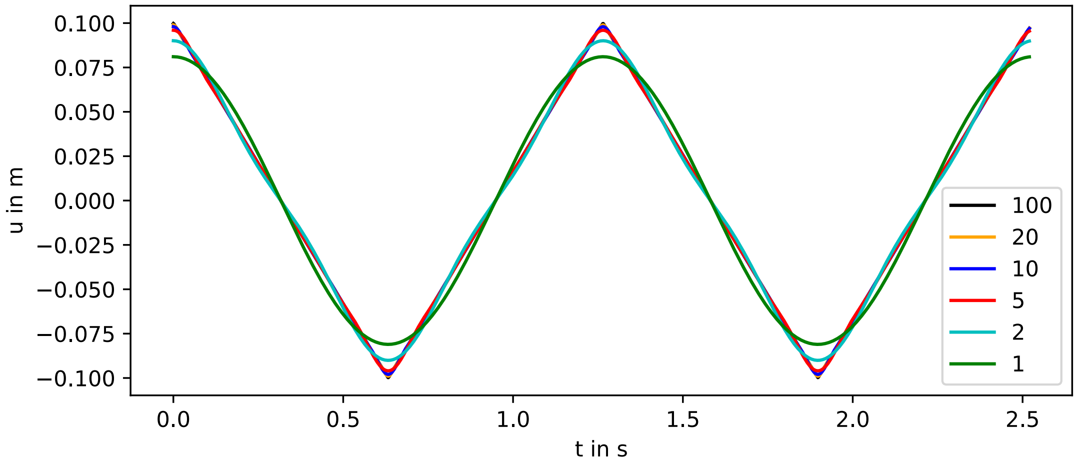

Figure 3: Approximations of the analytical solution with different numbers of summands.

The reference solution is set up with 50 spatial discretization points and 474 time steps which were chosen to ensure stability. The movement of the right end of the bar follows a sawtooth pattern which can be attributed to the initial condition of the system. The initial wave packet moves with constant shape back and forth through the bar. The oPINN is trained for 2000 epochs on collocation points with 50 spatial and 3000 time steps. The number of neurons is varied between one and 200.

The results obtained by oPINN with 20 neurons are compared to the analytical solution and the numerical reference solution in Fig. 4. Fig. 4 (left) shows that the reference solution achieves acceptable agreement with the analytical solution, but over the time of 10 seconds, a significan drift in the frequency builds up and a reduction of the amplitude corresponding to a significan numerical dissipation can be identified In opposition to that, the relative error of the amplitudes of the oPINN solution remains constant and amounts to 7.3%, while the shape of the displacement is in very good accordance with the expected sawtooth pattern. Moreover, the amplitude of the oPINN solution is constant and long-time stable, which has been additionally confirme by further studies on extended time intervals. The comparison of the calculated total energies is shown in Fig. 4 (right). The energies calculated from the oPINN and the analytic solution oscilla te arounda constant and stable mean value. These oscillations are comparatively small and most likely caused by numerical limitations during the postprocessing. The numerical reference solution, however, shows a significant monotonic decrease in the calculated total energy and thus exhibits significan numerical viscosity [12, 13, 11].

A comparison of results achieved with different numbers of neurons is shown in Fig. 5. The lowest frequency is always met with high accuracy and acceptable accuracy of amplitudes, while the increase of parameters allows the improvement of the fi at the peaks of the displacement curve. This indicates the applicability of oPINN with a reduced number of neurons directly as a tool for modal reduction.

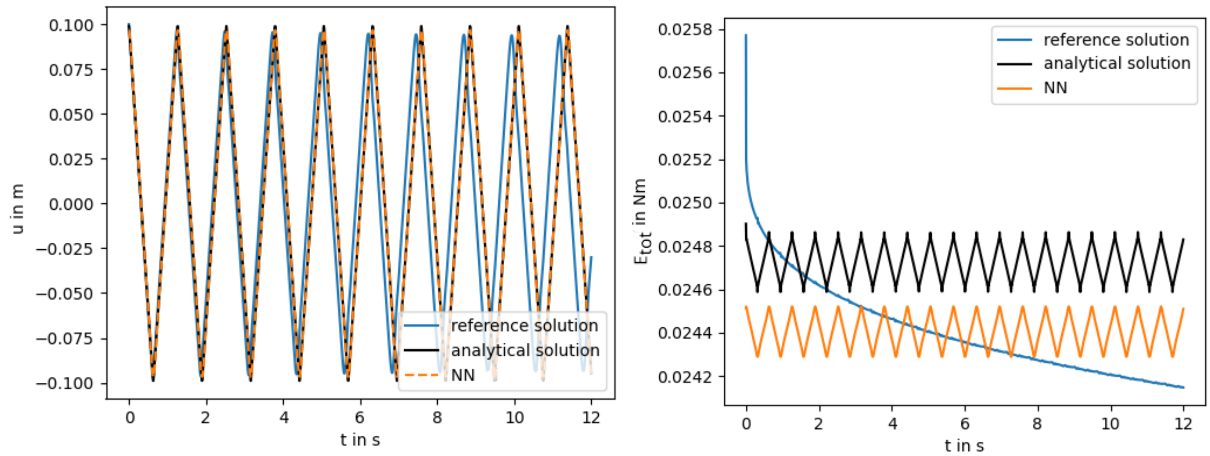

Figure 4: Comparison of the oPINN solution (20 neurons) with the numerical reference solution and the analytical solution. Comparison for the displacement of the point at the right end of the clamped bar (left). Comparison of the total energy (total sum of kinetic and potential energy) (right).

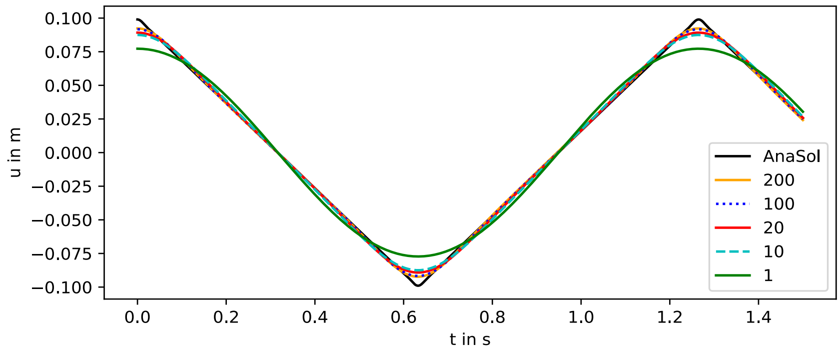

Figure 5: Comparison of the oPINN solution with different numbers of neurons and the analytical solution for the displacement of the point at the right end of the clamped bar.

6 CONCLUSIONS and OUTLOOK

In the current contribution, the new oPINN architecture for the analysis of vibrating structures with physics-informed neural networks has been presented. The architecture allows to combine the physical modeling of the system subject to analysis with several additional data sources, such as noisy or sparse measurement data, data-driven estimations and prior simulation results. At the same time, oPINN can be applied for modal analysis and modal reduction. The case study demonstrates the superiority of oPINN over conventional time-stepping algorithms. This is made possible by the two-sided temporal difference stencils and the search for the solution at the whole time interval of interest at once so that Dahlquist's barriers do not apply. The robustness of the method is underlined by the investigation on a case study that includes a sawtooth displacement curve with infinitel high frequencies.

In a future work, a more extensive investigation of the numerical properties of oPINN will be presented. Similarly, a combination of transfer learning with a rigorous hyperparameter optimization promises to significantl reduce the computational effort of the oPINN setup, especially for parameter studies and design optimization tasks and will be carried in future research. Finally, the application on two-dimensional and three-dimensional systems and adaptations for dissipative and nonlinear systems will be presented in future work.

REFERENCES

[1] Smetankina N, Pak A, Mandrazhy O, Usatova O and Vasiliev A 2023 Modelling of free axisymmetric vibrations of the fluid-fill shells with non-classical boundary interface conditions *Smart Technologies in Urban Engineering* ed Arsenyeva O, Romanova T, Sukhonos M, Biletskyi I and Tsegelnyk Y (Cham: Springer Nature Switzerland) pp 185–196 ISBN 978-3-031-46874-2

[2] Nicoletti R and Liebich R 2018 *Journal of Intelligent Material Systems and Structures* **29** 3108–3123 URL https://doi.org/10.1177/1045389X18783078

[3] Cicirello A 2024 *J. Phys.: Conf. Ser.* **2909** 012034 URL https://doi.org/10.1088/1742-6596/2909/1/012034

[4] Schilling G and Bäuerlein K and Liebich R 2019 *SIRM 2019 – 13th International Conference on Dynamics of Rotating Machines, Copenhagen, Denmark, 13th – 15th February 2019* URL https://www.static.tu.berlin/fileadmin/www/10002284/KuP/Forschen/Publikationen/SIRM2019_Numerical_Description_of_a_Rotor_supported_by_Gas_Polymer_Bearings.....pdf

[5] Pfeil S and Gravenkamp H and Duvigneau F and Woschke E 2023 *Int. J. Mech. Sc.* **247** 108164 URL https://doi.org/10.1016/j.ijmecsci.2023.108164

[6] Gräbner N and Tiedemann M and von Wagner Utz and Hoffmann N 2014 *SAE Technical Paper* URL https://doi.org/10.4271/2014-01-2511

[7] Stojanović V, Petković M D and Deng J 2018 *International Journal of Mechanical Sciences* **136** 155–168 ISSN 0020-7403 URL https://www.sciencedirect.com/science/article/pii/S0020740317317514

[8] Kranjc T, Slavič J and Boltežar M 2016 *Journal of Vibration and Control* **22** 371–381 URL https://doi.org/10.1177/1077546314533137

[9] Strzalka C 2023 *Untersuchungen zur modalen Superposition für die a priori Detektion versagenskritischer Regionen dynamisch beanspruchter Strukturen* Ph.D. thesis Technische Univesität Berlin

[10] Capuano G, Ruzzene M and Rimoli J J 2018 *Finite Elements in Analysis and Design* **145** 10–19 ISSN 0168874X

[11] Givoli D 2023 *J. Comp. Phys.* **475** 111836 URL https://doi.org/10.1016/j.jcp.2022.111836

[12] Hairer E and Wanner G 1996 *Solving Ordinary Differential Equations II: Stiff and Differential-Algebraic Problems* vol 14 (Berlin, Heidelberg: Scholars Portal) ISBN 978-3-642-05220-0

[13] Ghrist M L, Fornberg B and Reeger J A 2015 *BIT Numerical Mathematics* 1572–9125

[14] Tattersall P and McGuirk J 1994 *Computers & Fluids* **23** 177–209 ISSN 0045-7930 URL https://www.sciencedirect.com/science/article/pii/0045793094900345

[15] Karniadakis G E and Keyredikis I G and Lu L et al. 2021 *Nat. Rev. Phys.* **3** 422-440 URL `https://doi.org/10.1038/s42254-021-00314-5`

[16] Hildebrand S and Friedrich J G and Mohammadkhah M and Klinge S 2025 *Mach. Learn.: Sci. Technol.* **6** 015038 URL `https://doi.org/10.1088/2632-2153/adaf74`

[17] Le Clainche et al. 2023 *Aero. Sc. Tech.* 108354 URL `https://doi.org/10.1016/j.ast.2023.108354`

[18] Arabshahi F and Singh S and Anandkumar A 2018 *ICML workshop Neural Abstract Machines & Program Induction v2 (NAMPI)* URL `https://forougha.github.io/paperPDF/neuralODE_paper.pdf`

[19] Bock F E, Aydin R C, Cyron C J, Huber N, Kalidindi S R and Klusemann B 2019 *Frontiers in Materials* **6** ISSN 2296-8016 URL `https://www.frontiersin.org/articles/10.3389/fmats.2019.00110`

[20] Hildebrand S and Klinge S 2024 *Mach. Learn.: Sci. Technol.* **5** 045058 URL `https://iopscience.iop.org/article/10.1088/2632-2153/ad95da`

[21] Shoghi R and Morand L and Helm D and Hartmaier A 2024 *Comp. Mech.* **74** 447-466 URL `https://doi.org/10.1007/s00466-023-02440-6`

[22] Shoghi R and Hartmaier A 2024 *Mach. Learn.: Sci. Technol.* **5** 025008 URL `https://doi.org/10.1088/2632-2153/ad379e`

[23] Rezaei S, Moeineddin A and Harandi A 2024 *Computational Mechanics* **74** 333–366 ISSN 1432-0924

[24] Garai A and Haldar K 2025 *Int. J. Mech. Sc.* **286** 109860 URL `https://doi.org/10.1016/j.ijmecsci.2024.109860`

[25] Kalina K A et al. 2024 *Comp. Meth. App. Mech. Eng.* **421** 116739 URL `https://doi.org/10.1016/j.cma.2023.116739`

[26] Abdolazizi K P and Aydin R C and Cyron C J and Linka K 2025 *arXiv* URL `https://doi.org/10.48550/arXiv.2502.05682`

[27] Karabulut M 2025 *Buildings* **15**(3) 432 URL `https://doi.org/10.3390/buildings15030432`

[28] Raissi M, Perdikaris P and Karniadakis G 2019 *Journal of Computational Physics* **378** 686–707 ISSN 0021-9991 URL `https://www.sciencedirect.com/science/article/pii/S0021999118307125`

[29] Kollmannsberger S, D'Angella D, Jokeit M and Herrmann L 2021 *Deep Learning in Computational Mechanics* vol 977 (Cham: Springer International Publishing) ISBN 978-3-030-76586-6

[30] Braga-Neto U 2022 Characteristics-informed neural networks for forward and inverse hyperbolic problems URL `http://arxiv.org/pdf/2212.14012`

[31] Rodriguez-Torrado R, Ruiz P, Cueto-Felgueroso L, Green M C, Friesen T, Matringe S and Togelius J 2022 *Scientific reports* **12** 7557

[32] Coutinho E J R, Dall'Aqua M, McClenny L, Zhong M, Braga-Neto U and Gildin E 2023 *Journal of Computational Physics* **489** 112265 ISSN 00219991

[33] Samaniego E, Anitescu C, Goswami S, Nguyen-Thanh V M, Guo H, Hamdia K, Zhuang X and Rabczuk T 2020 *Computer Methods in Applied Mechanics and Engineering* **362** 112790 ISSN 00457825

[34] Mustajab A H, Lyu H, Rizvi Z and Wuttke F 2024 Physics-informed neural networks for high-frequency and multi-scale problems using transfer learning URL http://arxiv.org/pdf/2401.02810v2

[35] Rahaman N, Baratin A, Arpit D, Draxler F, Lin M, Hamprecht F A, Bengio Y and Courville A 2019 On the spectral bias of neural networks URL http://arxiv.org/pdf/1806.08734v3

[36] Rao S S 2019 *Vibration of Continuous Systems* (Wiley) ISBN 9781119424147

[37] Ramesh A and Utku S 1990 *Journal of Sound and Vibration* **139** 407–424 ISSN 0022-460X URL https://www.sciencedirect.com/science/article/pii/0022460X9090673N

[38] Hagedorn P and DasGupta A 2007 *Vibrations and Waves in Continuous Mechanical Systems* (Wiley) ISBN 9780470517383

[39] Abueidda D W, Lu Q and Koric S 2021 *International Journal for Numerical Methods in Engineering* **122** 7182–7201

[40] Hornik K 1991 *Neural Networks* **4** 251–257 ISSN 0893-6080 URL https://www.sciencedirect.com/science/article/pii/089360809190009T

[41] Kingma D P and Ba J 2014 Adam: A method for stochastic optimization URL http://arxiv.org/pdf/1412.6980v9

[42] Stender M, Tiedemann M, Spieler D, Schoepfli D, Hoffmann N and Oberst S 2021 *Mechanical Systems and Signal Processing* **149** 107181 ISSN 0888-3270 URL https://www.sciencedirect.com/science/article/pii/S0888327020305677

[43] Wulff P, Lentz L and von Wagner U 2023 *Acta Mechanica* **234**(5) 1973–1989

[44] Zamfirach I A, Precup R E and Petriu E M 2023 *Facta Universitatis* **21**(4) 615–630

[45] Mohaghegh F, Murthy J and Alam M R 2021 *Applied Ocean Research* **117** 102920 ISSN 0141-1187 URL https://www.sciencedirect.com/science/article/pii/S0141118721003886

[46] Hildebrand S and Klinge S 2024 *Neural Computing and Applications* **36** 16657-16682 URL https://doi.org/10.1007/s00521-024-10132-2

[47] Herrmann L and Kollmannsberger S 2024 *Computational Mechanics* ISSN 0178-7675

[48] Nguyen-Thanh V M, Zhuang X and Rabczuk T 2020 *European Journal of Mechanics - A/Solids* **80** 103874 ISSN 09977538

[49] He J, Chadha C, Kushwaha S, Koric S, Abueidda D and Jasiuk I 2023 *Acta Mechanica* **234**(4) 1365–1379 URL https://doi.org/10.1007/s00707-022-03449-3

[50] Zeng Q, Kothari Y, Bryngelson S H and Schäfer F 2022 Competitive physics informed networks URL https://arxiv.org/abs/2204.11144

[51] Radin N, Klinkel S and Altay O 2023 *PAMM* **23**

[52] Chadha C, He J, Abueidda D, Koric S, Guleryuz E and Jasiuk I 2023 *Acta Mechanica* **234** 5975–5998 ISSN 0001-5970

[53] Berrone S, Canuto C, Pintore M and Sukumar N 2023 *Heliyon* **9** e18820 ISSN 2405-8440

[54] Kleinberg R, Li Y and Yuan Y 2018 An alternative view: When does sgd escape local minima? URL http://arxiv.org/pdf/1802.06175v2

[55] You K, Long M, Wang J and Jordan M I 2019 How does learning rate decay help modern neural networks? URL http://arxiv.org/pdf/1908.01878